

# Influence of Flexible Oligo(tetrafluoroethene) Segment on the Sorption and Diffusion of Carbon Dioxide in Poly(amide-imide) Membranes

Yu Chen, Shu Ping Huang, Qing Lin Liu, Ian Broadwell, Ai Mei Zhu

National Engineering Laboratory for Green Chemical Productions of Alcohols, Ethers, and Esters, The College of Chemistry and Chemical Engineering, Xiamen University, Xiamen 361005, China

Received 15 May 2010; accepted 12 September 2010

DOI 10.1002/app.33411

Published online 1 December 2010 in Wiley Online Library (wileyonlinelibrary.com).

**ABSTRACT:** Molecular simulations have been used to study the sorption and diffusion properties of carbon dioxide in a series of poly (amide-imide) (PAI) membranes containing oligo(tetrafluoroethene) segment with various numbers ( $n = 0, 1, 2, 3,$  and  $4$ ) of tetrafluoroethene units. The solubility and self-diffusion coefficients were computed by the Grand Canonical Monte Carlo (GCMC) method and molecular dynamics (MD) simulations respectively. It was found that increasing the fluorine content of the polymer membrane reduced the associated glass transition temperature ( $T_g$ ) and led to an increase in diffusion coefficient of carbon dioxide. Results indicate that pene-

trant molecule's diffusion coefficient is strongly dependent on chain mobility. It is also noticed that the radial distribution functions (RDFs) are inconsistent with the  $d$ -spacings of PAIs calculated from X-ray data. This is also thought to be tied to the number of degrees of freedom of the chain. Finally, this study gives a useful insight into how PAIs with high fluorine content can be tailored with a high permeability to carbon dioxide. © 2010 Wiley Periodicals, Inc. *J Appl Polym Sci* 120: 1859–1865, 2011

**Key words:** molecular dynamics simulations; poly(amide-imide); membranes; sorption; diffusion

## INTRODUCTION

Poly (amide-imide)s (PAIs) are a well known class of polymers which display a useful range of material properties such as high thermal stability, ease of processing and chemical resistance to harsh solvents. These features make PAIs particularly useful in demanding fuel cell environments where compromises often have to be made between cost of the membrane material and actual performance.

In recent years gas transport through polymer films has been one of the major areas of interest. With increasing demand for the use of synthetic polymers in engineering, medicine, separation science and food packaging, a range of different polymer backbones exhibiting superior transport properties have been synthesized. PAIs are one such example of this recent

research effort<sup>1,2</sup> and particularly used as a membrane for CO<sub>2</sub> separation<sup>3,4</sup> to meet the requirement for low CO<sub>2</sub> emission. The current body of knowledge regarding PAIs can be broadly divided into three areas which include: (1) synthesis, (2) modification, and (3) structure determination. Despite the numerous experimental studies which have been performed to date and the observations that: introduction of favorable functional groups onto the polymer backbones during synthesis of aromatic PAIs enhances gas transport (e.g., CO<sub>2</sub> diffusion),<sup>5–9</sup> there still remains a lack of understanding about the structural dependence of sorption and diffusion of small molecules in PAIs.

The rapid development of computational science has provided the tools to establish structure–property relationships through molecular simulations. Such simulations allow one to gain a better understanding of the transport mechanism of small molecules at the microscopic level. Modeling studies can be classed as a first step to designing innovative materials which possess the right material properties for use in a specific application. Molecular dynamics (MD) studies on sorption and diffusion of gases including carbon dioxide in polymer membranes have been reported for a long time. For example, Pavel et al.<sup>10,11</sup> studied diffusion of O<sub>2</sub> and CO<sub>2</sub> in amorphous poly(ethylene terephthalate) and related aromatic polyesters. Mozaffari et al.<sup>12</sup> studied the

Correspondence to: Q. L. Liu (qlliu@xmu.edu.cn).

Contract grant sponsor: National Nature Science Foundation of China; contract grant numbers: 20976145, 21076170.

Contract grant sponsor: Nature Science Foundation of Fujian Province of China; contract grant number: 2009J01040.

Contract grant sponsor: Doctoral Program of Higher Education; contract grant number: 20090121110031.

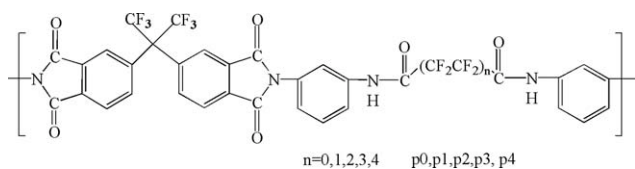


**Figure 1** Repeat units of poly(amide-imide)s containing oligo(tetrafluoroethene).

diffusion and permeation of gases including argon, nitrogen, methane, carbon dioxide, and propane in polystyrene over a wide range of temperatures. A jumping mechanism is observed for the diffusion of diffusants in polymer. Takaba et al.<sup>13</sup> studied the dynamic behavior of the separation of CO<sub>2</sub> from the CO<sub>2</sub>/N<sub>2</sub> gas pair in inorganic membranes at high temperatures.

Until now, only a few molecular simulations of PAIs have been reported. Most of the studies reported so far have dealt with theoretical aspects of modeling polyimides and polyamides. For example, Hofmann et al.<sup>14</sup> studied the transport of small molecules in the stiff chain glassy polyimide and polyamide. Pan et al.<sup>15</sup> applied atomic modeling techniques to three polyimides with different methylene spacing groups in biphenyl side chains, to reveal the structure–property relationship of polyimide. Neyertz et al.<sup>16–18</sup> investigated the effects of system size, different dianhydride and diamine on the diffusion of gas molecules, and the mobility modes of gas. Sridhar et al.<sup>19</sup> performed molecular dynamics simulations to compute the sorption of CO<sub>2</sub>, H<sub>2</sub>S, CH<sub>4</sub>, O<sub>2</sub>, and N<sub>2</sub> gases in polyamide membrane to corroborate the theoretical study with experimentally determined gas transport properties.

This creates an opportunity for investigating PAI materials. Some limited body of work in this area does exist. Richeton et al.<sup>20</sup> modeled the compressive stress of PAI; Schmidtke et al.<sup>21</sup> adopted an improved method to describe the unoccupied volume in PAI by probing it with a tracer atom. Hofmann et al.<sup>22</sup> investigated the transport of different gases in a PAI and two polyimides (PI) using molecular dynamic simulations. It has been reported that the difference between the PAIs and PIs is that PAIs have broader and more permanent structure channels.

In our previous study, the structure dependence of diffusion properties of PAIs with para- and meta-substitutions and diffusivity/selectivity toward CO<sub>2</sub>/CH<sub>4</sub> pair were investigated.<sup>23</sup> In this work, atomistic simulation techniques are adopted to make predictions about the physical properties of PAIs. We focus on fundamentally understanding the structure-property relationships of a series of PAIs with different lengths of oligo(tetrafluoroethene) segments. The density, fractional free volume, and glass transition temperature of the polyamide-imides were calculated

to investigate the microstructure of the polyamide-imides and the structure dependence of permeation properties of CO<sub>2</sub>. The effect of fluorine content on the diffusion and sorption is investigated by the MD and GCMC methods, respectively. Hence, this study may provide a guideline for designing complex aromatic polyamide-imides membranes to have tailored properties.

## MODEL AND SIMULATION DETAILS

### Model construction

Molecular mechanics (MM) and MD simulations have been carried out using commercial software of Materials Studio (Accelrys). The COMPASS force field,<sup>24</sup> which provides an excellent potential model for many polymers,<sup>25,26</sup> is adopted to conduct computations. Three-site model is used to represent the CO<sub>2</sub> molecules.

The chemical structures of the repeat unit of poly(amide-imide)s containing different length of oligo(tetrafluoroethene) segments<sup>27</sup> used in this study are shown in Figure 1. The poly(amide-imide)s used in this work were designated as pn ( $n = 0, 1, 2, 3,$  and  $4$ ), where  $n$  is the number of tetrafluoroethene units (see Fig. 1). The chain end groups have been saturated by the H atoms and their physical properties are listed in Table I.

Utilizing the amorphous-cell module, which implements a modification of the self-avoiding random-walk (RIS) method of Theodorou and Suter,<sup>28,29</sup> a polymer chain with 40 repeating monomer units (up to 3600 atoms, Table II) was constructed (grown atom by atom) under the periodic boundary conditions at 308 K. Attempts failed to construct the cell at a high density and there were no experimental densities available, so an initial density of 0.1 g cm<sup>-3</sup>

**TABLE I**  
Characteristics of PAIs Containing  
Oligo(tetrafluoroethene) Used in this Study<sup>27</sup>

Polymer	Formula	$T_g$ (K) <sup>a</sup>	$\eta_{inh}$ (g cm <sup>-3</sup> ) <sup>b</sup>	Fluorine content (wt %) <sup>c</sup>
p0	C <sub>33</sub> H <sub>14</sub> F <sub>6</sub> N <sub>4</sub> O <sub>6</sub>			
p1	C <sub>35</sub> H <sub>14</sub> F <sub>10</sub> N <sub>4</sub> O <sub>6</sub>			24.5
p2	C <sub>37</sub> H <sub>14</sub> F <sub>14</sub> N <sub>4</sub> O <sub>6</sub>	558	0.83	30.3
p3	C <sub>39</sub> H <sub>14</sub> F <sub>18</sub> N <sub>4</sub> O <sub>6</sub>	538	0.86	35.0
p4	C <sub>41</sub> H <sub>14</sub> F <sub>22</sub> N <sub>4</sub> O <sub>6</sub>			

<sup>a</sup>  $T_g$  was determined by dynamic mechanical analysis (DMA) using a Rheometric Solid Analyser RSAII at a heating rate of 10 K min<sup>-1</sup> and an oscillation frequency of 1 Hz.

<sup>b</sup> Inherent viscosities were determined at 303.15 K in DMF at concentrations of 0.5 g L<sup>-1</sup>.

<sup>c</sup> Fluorine content is taken from experimental value in literature.<sup>27</sup> There is no P0 and P4 values available in literature, since they are polymers designed for studying the influence of oligo(tetrafluoroethene) segments.

TABLE II  
The Model Parameters Under 308 K

Polymer	Number of atom	Cell lengths (Å)	$T_g^{\text{Exp. } 30}$ (K)	$T_g^{\text{Cal.}}$ (K)	$d$ -spacing (Å)
p0	2602	31.47		640 ± 5	5.82 ± 0.04
p1	2842	32.83		603 ± 2	5.69 ± 0.03
p2	3082	33.91	558.25	563 ± 5	5.51 ± 0.02
p3	3322	34.83	538.25	543 ± 2	5.75 ± 0.06
p4	3562	35.57		525 ± 5	5.97 ± 0.07

was adopted.<sup>31</sup> For each PAI, 20 configurations were independently generated and the three configurations that had the lowest energy were chosen to endure the subsequent equilibration procedure, in which the cells change freely. About 500 ps NPT (at 1 atm) and 500 ps NVT MD simulations were first performed at 600 K to relax the unfavorable overlaps, and then conducted at 308 K for 200 ps. The resulting cells were subsequently minimized by performing NPT MD simulations at 1 atm using an annealing dynamics program (Temperature-cycle, Amorphous-cell). During annealing, the cells were first heated by 50 K increments from 300 to 700 K and then cooled back to 300 K. The duration of the NPT MD simulations at each temperature was 150 ps. The structures were finally subjected to a 200 ps NVT MD simulation at 308 K to equilibrate the structures. The length of the resulting equilibrium cell is given in Table II.

The Andersen and Berendsen methods<sup>32,33</sup> were adopted in all the simulation for controlling the temperature and pressure. The nonbonded interactions including van der Waals and Coulmbic were both taken into account. The former was calculated using the atom-based technique with a cutoff of 12.5 Å, and the latter; estimated using the Ewald summation method. The Ewald summation parameters were set with an accuracy of 0.001 kcal mol<sup>-1</sup>(separation parameter  $\alpha = 0.21 \text{ \AA}^{-1}$ ), update width of 3.00 Å (determined by MS) and time step of 1 fs.

### Simulation of $T_g$ , diffusion and sorption

Optimized configurations at 308 K were first made for each different polymer having previously been gently heated to temperatures of 700 or 750 K (p0 and p1: 750 K; p2, p3 and p4: 700 K). Configurations were then kept at those temperatures for 200 ps under the NVT ensemble. Thereafter, the systems were cooled down under NPT ensemble to temperature of 400 or 450 K (p0 and p1: 450 K; p2, p3, and p4: 400 K) by 25 K steps of 250-ps duration each, giving a cooling rate of  $6 \times 10^{12} \text{ K min}^{-1}$ . The  $T_g$ s of the PAIs were obtained from the specific volume curve at the point of intersection of two piecewise linear fits.

Diffusion coefficients were estimated to understand the diffusion characteristics of gas molecules in polymer containing different lengths of oligo(tetrafluoroethene) segments in the diamine moiety. Ten CO<sub>2</sub> molecules were inserted into each equilibrated PAI microstructure, and the resulting structure was then equilibrated using the same procedure outlined above. The averaged center of mass diffusion coefficients of all penetrant molecules can be calculated using the Einstein equation<sup>34</sup> via a 3 ns-NVT MD simulation at 308 K.

The solubility coefficient of CO<sub>2</sub> in equilibrated PAIs was obtained from the sorption isotherms<sup>26</sup> by the GCMC method. The calculations were carried out on a single configuration snapshot of the packing models, i.e., the position of matrix atoms was fixed. The calculated concentration therefore resembles a "hole filling" without taking into account the swelling of the matrix. The program uses a Metropolis algorithm<sup>35</sup> for verifying the validity of molecular/atomic configurational moves and also allows for insertion or deletion of sorbates. Both van der Waals and Coulombic forces were considered in the computation of sorption. The cutoff used for the estimation of nonbonded interaction was set to 12.5 Å and the pressure was increased from 0.1 to 10 atm. At each pressure, 1,000,000 steps of GCMC calculations were performed using an initial equilibration period of 100,000 steps.

## RESULTS AND DISCUSSION

### Calculation of $T_g$ values

The simulated  $T_g$  values of PAIs containing oligo(tetrafluoroethene) segment are listed in Table II. The simulated values of  $T_g$  of p2 and p3 are in agreement with the experimental values obtained by dynamic mechanical analysis,<sup>30</sup> although, systematically higher than the experimental ones as expected. This is probably due to the fast cooling rates of  $6 \times 10^{12} \text{ K min}^{-1}$  used in the MD simulations.<sup>36,37</sup> It is found that the  $T_g$  decreased with increasing length of oligo(tetrafluoroethene) segment incorporated into the main chain of the PAIs, as noted by Schneider et al.<sup>27</sup> This is probably due to the fact that extending the oligo(tetrafluoroethene) segment

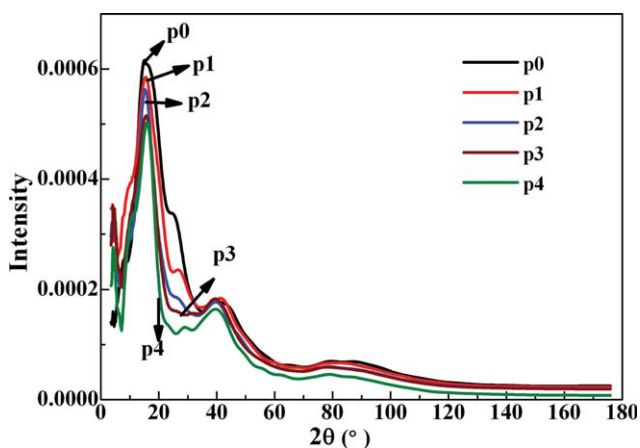


**Figure 2** Simulated X-ray diffraction patterns of poly(amide-imide)s. [Color figure can be viewed in the online issue, which is available at [wileyonlinelibrary.com](http://wileyonlinelibrary.com).]

increases the segmental mobility and the conformational freedom.

### X-ray diffraction and RDF

To understand the structure of the PAI in the presence of different length of oligo(tetrafluoroethene) segments, the X-ray diffraction patterns (a plot of intensity versus the scattering angle,  $2\theta$ ) were computed using the Discover module in the MS software suite. The X-ray patterns of PAIs show broad peaks around  $2\theta = 16^\circ$ , which corresponds to the interchain distances ( $d$ -spacing) of  $\sim 5.7$  Å. Diffraction patterns of PAIs (Fig. 2) show that the peak intensity progressively decreased from p0 to p4.

The radial distribution function (RDF),  $g(r)$ , can provide an insight into the microstructure of the material.<sup>38</sup> The RDFs shown in Figure 3 are calcu-

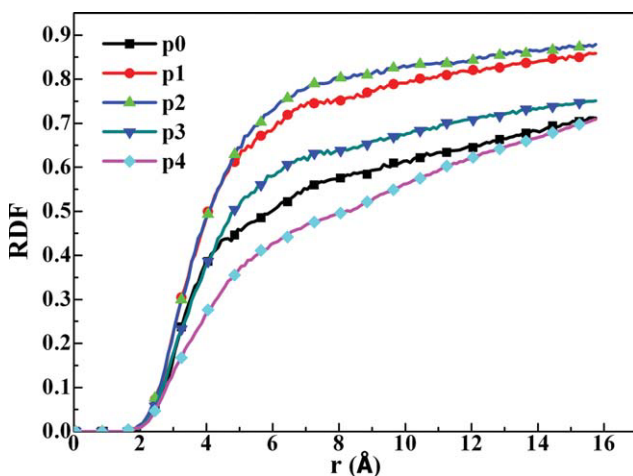


**Figure 3** The intermolecular RDFs at 308 K based on all the carbon atoms of poly(amide-imide)s. [Color figure can be viewed in the online issue, which is available at [wileyonlinelibrary.com](http://wileyonlinelibrary.com).]

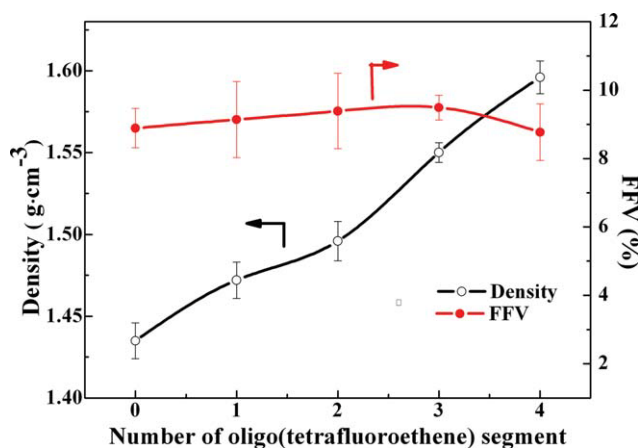


**Figure 4** The simulated density and FFV of poly(amide-imide)s probed by  $\text{CO}_2$ . [Color figure can be viewed in the online issue, which is available at [wileyonlinelibrary.com](http://wileyonlinelibrary.com).]

lated for each individual PAI molecule type and consider the individual contribution of all carbon atoms based in that sample. Each PAI exhibits a diffuse peak of  $\sim 5$ – $6$  Å, corresponding to its average interchain spacing. The  $g(r)$  values first increased from p0 to p2, and then decreased. This is consistent with the  $d$ -spacing values listed in Table II. However, slight differences in the average interchain spacing are observed for this series of PAIs. Increasing the length of oligo(tetrafluoroethene) segment from 2 to 4 results in a decrease in the  $g(r)$  value. This may be because the polar  $\text{CF}_2$  groups cause significant inter-ring repulsions and push the chains apart, thus reduce the number of interchain contacts.

### Density and fractional free volume

Compared with those similar polyimides and poly(amide-imide)s<sup>5,39,40</sup> which report no experimental data of PAI densities, the calculated density seems reasonable (Fig. 4). The density increases with extending oligo (tetrafluoroethene) segment which affects the flexibility of the PAIs, and thus increases the chain packing efficiency.

Free volume plays a crucial role in the transport behavior of penetrant molecules in membranes. Atoms of the PAI membranes are represented by hard spheres each having an associated van der Waals radius. The penetrant molecule,  $\text{CO}_2$ , is chosen as the probe molecule and is modeled by a sphere with radius of 1.65 Å. The Connolly surface is calculated using the technique reported by Zhang et al.<sup>41</sup> The simulated fractional free volume (FFV) of the PAI membranes probed by  $\text{CO}_2$  is shown in Figure 4. The FFV first appears to increase with length of oligo(tetrafluoroethene) segment on the main chain, then decreased above 3 oligo(tetrafluoroethene) segments. Based on the errors and negligible statistical differences no firm trend can be concluded.

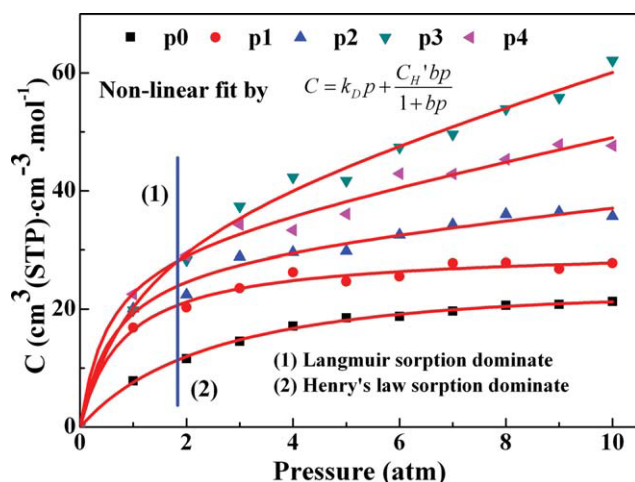


**Figure 5** Simulated sorption isotherm of CO<sub>2</sub> at 308 K. [Color figure can be viewed in the online issue, which is available at [wileyonlinelibrary.com](http://wileyonlinelibrary.com).]

### Sorption

As we cannot really see the plasticization effects, we checked the tensile module of two polymers with and without gas molecules inserting. The tensile module of p2 without gas molecules is 3.76 GPa, whereas with gases is 3.19 GPa. The higher tensile module of the cell without gases than that with gases was also noted for p3 (3.56/2.92). This may indicate the plasticization effects on the polymer chains.

The solubility coefficient characterizes the interaction between a penetrant and a polymer, and is associated with the amount of the penetrant that can be accommodated in the polymer at equilibrium. Representative sorption isotherms obtained from GCMC simulation for gas in glassy PAIs are shown in Figure 5. Averaged solubility coefficients at 10 atm obtained from the isotherms of each equilibrated configuration are listed in Table III. The simulated solubility coefficients of p2 and p3 (Table III) are close to the reported experimental values of [4.58 cm<sup>3</sup> (STP) cm<sup>-3</sup> (polymer) atm<sup>-1</sup> for p2 and 5.84 cm<sup>3</sup> (STP) cm<sup>-3</sup> (polymer) atm<sup>-1</sup> for p3 at 10 atm].<sup>30</sup> As shown in Figure 6, the solubility coefficient first increased with increasing length of oligo(tetrafluoroethene) segments in the main chain, then clearly decreased above 3 oligo(tetrafluoroethene) segments. This is because the incorporation of oligo(tetrafluoroethene) segments induces an increase in

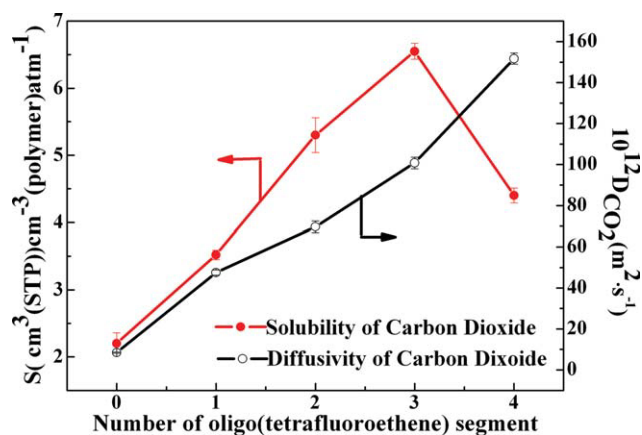


**Figure 6** The relationships between solubility coefficients, diffusion coefficients and fluorine content. [Color figure can be viewed in the online issue, which is available at [wileyonlinelibrary.com](http://wileyonlinelibrary.com).]

favorable quadrupole–dipole interactions between CO<sub>2</sub> and the fluoroalkyl groups.<sup>34,42</sup> In addition, the incorporation of the segments increases the FFV in the PAIs, thus resulting in an increased solubility of the penetrant gas. With the insertion of more than three segments in the main chain, the solubility of p4 can be seen to decrease. This is thought to be due to the increased packing density associated with higher pn.

### Diffusion

The diffusivities and the mean-square displacement (MSD) of CO<sub>2</sub> in PAI membranes are shown in Table III and Figure 7, respectively. Taking p3 as an example, it is found that the slope of the plot is 0.75 within 200 ps, suggesting an anomalous diffusion (Fig. 8). Afterward, the slope increases to unity, indicating a normal diffusion of CO<sub>2</sub>. The diffusion coefficients of CO<sub>2</sub> can thus be calculated using the Einstein equation.

Although the simulation has been run for 3 ns, the simulated diffusivities of CO<sub>2</sub> in p2 and p3 in the present work are nearly two orders of magnitude larger than previously reported experimental values (95 and 116 × 10<sup>-10</sup> cm<sup>2</sup> s<sup>-1</sup>).<sup>30</sup> Heuchel et al.<sup>43</sup> and Lim et al.<sup>44</sup> have also encountered difficulties with CO<sub>2</sub>, since the values of the diffusion coefficients are extremely small (~ 10<sup>-13</sup> m<sup>2</sup> s<sup>-1</sup>). As is well-known,

**TABLE III**  
The Simulated Solubility Coefficients and Diffusion Coefficients

	p0	p1	p2	p3	p4
$S$ [cm <sup>3</sup> (STP) cm <sup>-3</sup> (polymer)atm <sup>-1</sup> ]	2.20 ± 0.16	3.52 ± 0.07	5.30 ± 0.26	6.55 ± 0.12	4.91 ± 0.62
$D_{\text{CO}_2}$ 10 <sup>-12</sup> m <sup>2</sup> s <sup>-1</sup>	8.48 ± 0.25	47.5 ± 1.3	69.7 ± 2.8	100.8 ± 2.8	151.7 ± 2.7
$D_{\text{backbone}}$ 10 <sup>-12</sup> m <sup>2</sup> s <sup>-1</sup>	0.09 ± 0.03	0.12 ± 0.02	0.25 ± 0.04	0.76 ± 0.11	0.93 ± 0.06

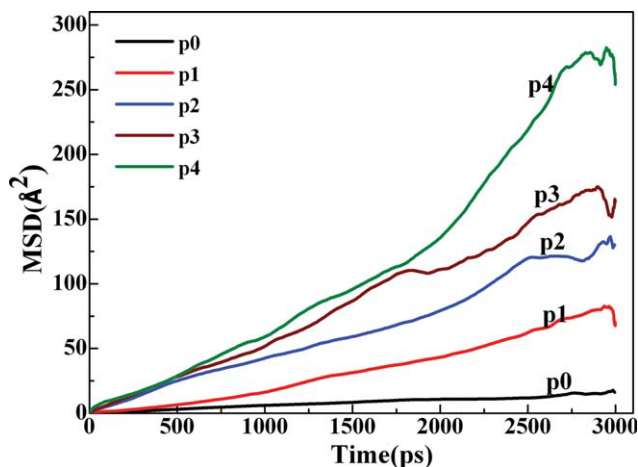


**Figure 7** The simulated MSD curves of PAIs. [Color figure can be viewed in the online issue, which is available at [wileyonlinelibrary.com](http://wileyonlinelibrary.com).]

obtaining reasonable  $D$  values by computer simulation depends on many factors; such as the simulation time, the cutoff used for nonbonded interactions as well as other assumptions and approximations included in the MD simulations.<sup>45</sup> For example, the parameters of the COMPASS force field have been optimized for accurate representation of the polymer's morphology, not optimized for the transport properties of gas molecules in the polymer. In addition, these parameters have not been optimized based on any data for diffusion of gas molecules in the polymer. These facts suggest that the same optimized parameters (for the polymer's morphology) do not necessarily provide accurate estimation of the diffusivity of the gas molecules in the polymers. Besides, there is also a possibility that the gases inserted are not fully dissolved into the polymer, which results in the higher diffusion coefficients. It

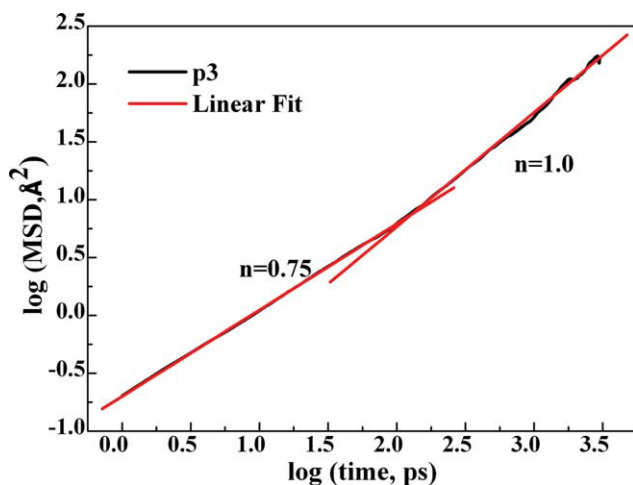


**Figure 8**  $\log(\text{MSD})$  versus  $\log(t)$  plot for the diffusion of  $\text{CO}_2$  in p3. [Color figure can be viewed in the online issue, which is available at [wileyonlinelibrary.com](http://wileyonlinelibrary.com).]

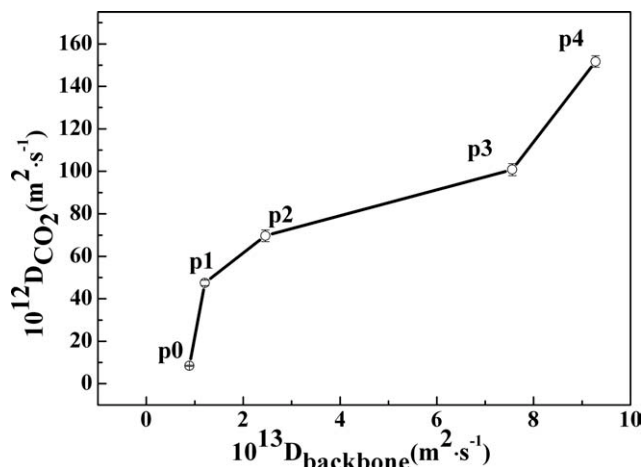


**Figure 9** The effect of flexibility of the polymer backbone on diffusivities of gas.

should be pointed out that experimental observation normally yields mutual-diffusion coefficients instead of the self-diffusion coefficients. Here, our focus is mainly on the trends of diffusivity of small penetrants in different kinds of PAI membranes. We noted that the simulated ratio of  $D_{p3}/D_{p2} = 1.44$  is relatively close to the experimental value of 1.22.<sup>30</sup> Moreover, the diffusivity of  $\text{CO}_2$  increases as the number of flexible oligo(tetrafluoroethene) segments on the main chain increases (Fig. 6).

The permeability of a polymer membrane depends on the length of diffusion paths penetrant molecules take. The modeling of these paths and transport properties is central to this theoretical study since diffusion coefficients depend on chain length and mobility. The polymer chains' mobility has been investigated by analyzing the MSD and the results are listed in Table III. Figure 9 shows the effect of chain flexibility on diffusion coefficients. The diffusivity of  $\text{CO}_2$  increased with increasing chain mobility and the enhancement of chain mobility is found to be consistent with the decrease trend of  $T_g$  and X-ray diffraction intensity. The difference in FFV of the polymers, as the other factor affects the gas diffusion, as discussed above, is not significant. One can thus conclude that an increase in the  $\text{CO}_2$  diffusivities with increasing oligo(tetrafluoroethene) segment length is mainly attributed to the chain mobility. The results show that the insertion of flexible groups is beneficial for synthesis of membranes with a high permeability to carbon dioxide.

## CONCLUSION

Molecular simulations have been used to study the gas sorption, diffusion, and other properties of a series of poly (amide-imide) membranes containing different numbers of oligo(tetrafluoroethene) segments.

A significant increase in the chain mobility with increasing length of oligo(tetrafluoroethene) segments on the main chain of PAI was observed and characterized by the associated glass transition temperature.

The approach used in this work provides some insight into the microstructure and dynamics properties for these PAIs. The solubility coefficient was noted first to increase with increasing oligo(tetrafluoroethene) segments on the main chain, then to decrease above 3 oligo(tetrafluoroethene) segments. This decrease in the solubility thought to be due to a decrease in free volume that can be occupied by CO<sub>2</sub>. The incorporation of flexible oligo(tetrafluoroethene) segments was found to result in an increase of CO<sub>2</sub> diffusivities. This study serves as a first step in the design of new poly(amide-imide)s membranes with high fluorine content which exhibit a high degree of permeability to carbon dioxide. We believe that through additional theoretical simulations of chain mobility further material improvements can be made.

Computing services provided by the 985 computer center (Xiamen University) is acknowledged.

## References

1. Kucukpinar, E.; Doruker, P. *Polymer* 2003, 44, 3607.
2. Comyn, J. *Polymer Permeability*, 2nd Ed.; Chapman & Hall: London, 1994.
3. Hu, Q.; Marand, E.; Dhingra, S.; Fritsch, D.; Wen, J.; Wilkes, G. *J Membr Sci* 1997, 135, 65.
4. Langsam, M.; Laciak, D. V. *J Polym Sci A Polym Chem* 2000, 38, 1951.
5. Huang, S. H.; Hu, C. C.; Lee, K. R.; Liaw, D. J.; Lai, J. Y. *Eur Polym J* 2006, 42, 140.
6. Mehdipour-Ataei, S.; Zighemat, F. *Eur Polym J* 2007, 43, 1020.
7. Kosuri, M. R.; Koros, W. *J Membr Sci* 2008, 320, 65.
8. Wang, Y.; Goh, S. H.; Chung, T. S.; Na, P. *J Membr Sci* 2009, 326, 222.
9. Shockravi, A.; Abouzari-Lotf, E.; Javadi, A.; Atabaki, F. *Eur Polym J* 2009, 45, 1599.
10. Pavel, D.; Shanks, D. *Polymer* 2003, 44, 6713.
11. Pavel, D.; Shanks, D. *Polymer* 2005, 46, 6135.
12. Mozaffari, F.; Eslami, H.; Moghadasi, J. *Polymer* 2010, 51, 300.
13. Takaba, H.; Mizukami, K.; Kubo, M.; Stirling, A.; Miyamoto, A. *J Membr Sci* 1996, 121, 251.
14. Hofmann, D.; Fritz, L.; Ulbrich, J.; Schepers, C.; Bohning, M. *Macromol Theory Simul* 2000, 9, 293.
15. Pan, R.; Liu, X.; Zhang, A.; Gu, Y. *Comput Mater Sci* 2007, 39, 887.
16. Neyertz, S.; Brown, D. *Macromolecules* 2004, 37, 10109.
17. Neyertz, S. *Macromol Theory Simul* 2007, 16, 513.
18. Neyertz, S.; Brown, D. *Macromolecules* 2008, 41, 2711.
19. Sridhar, S.; Smitha, B.; Satyajai, M.; Prathab, B.; Aminabhavi, T. M. *J Mater Sci* 2007, 42, 9392.
20. Richeton, J.; Ahzi, S.; Vecchio, K. S.; Jiang, F. C.; Adharapurapu, R. R. *Int J Solids Struct* 2006, 43, 2318.
21. Schmidtke, E.; Günther-Schade, K.; Hofmann, D.; Faupel, F. *J Mol Graph Model* 2004, 22, 309.
22. Hofmann, D.; Ulbrich, J.; Fritsch, D.; Paul, D. *Polymer* 1996, 37, 4773.
23. Chen, Y.; Liu, Q. L.; Zhu, A. M.; Zhang, Q. G.; Wu, J. Y. *J Membr Sci* 2010, 348, 204.
24. Sun, H. *J Phys Chem B* 1998, 102, 7338.
25. Wang, X. Y.; Raharjo, R. D.; Lee, H. J.; Lu, Y.; Freeman, B. D.; Sanchez, I. C. *J Phys Chem B* 2006, 110, 12666.
26. Heuchel, M.; Fritsch, D.; Budd, P. M.; McKeown, N. B.; Hofmann, D. *J Membr Sci* 2008, 318, 84.
27. Schneider, H. A.; Stein, H. N.; Müllhaupt, R. *Polym Bull* 1994, 32, 339.
28. Theodorou, D. N.; Suter, U. W. *Macromolecules* 1985, 18, 1467.
29. Theodorou, D. N.; Suter, U. W. *Macromolecules* 1986, 19, 139.
30. Xu, Z. K.; Böhring, M.; Springer, J.; Steinhauser, N.; Müllhaupt, R. *Polymer* 1997, 38, 581.
31. Liu, Q. L.; Huang, Y. *J Phys Chem B* 2006, 110, 17375.
32. Andersen, H. C. *J Chem Phys* 1980, 72, 2384.
33. Berendsen, H. J. C.; Postama, J. P. M.; van Gunsteren, W. F.; Dinola, A.; Haak, J. R. *J Chem Phys* 1984, 81, 3684.
34. Neyertz, S. *Soft Mater* 2007, 4, 15.
35. Metropolis, N.; Rosenbluth, A. W.; Rosenbluth, M. N.; Teller, A. H.; Teller, E. *J Chem Phys* 1953, 21, 1087.
36. Paul, W. *Polymer* 2004, 45, 3901.
37. Buchholz, J.; Paul, W.; Varnik, F.; Binder, K. *J Chem Phys* 2002, 117, 7364.
38. Chang, K. S.; Hsiung, C. C.; Lin, C. C.; Tung, K. L. *J Phys Chem B* 2009, 113, 10159.
39. Mi, Y. S.; Stern, A.; Trohalaki, S. *J Membr Sci* 1993, 77, 41.
40. Matsumoto, K.; Xu, P.; Nishikimi, T. *J Membr Sci* 1993, 81, 15.
41. Zhang, Q. G.; Liu, Q. L.; Chen, Y.; Wu, J. Y.; Zhu, A. M. *Chem Eng Sci* 2009, 64, 334.
42. Fried, J. R.; Hu, N. *Polymer* 2003, 44, 4363.
43. Heuchel, M.; Hofmann, D.; Pullumbi, P. *Macromolecules* 2004, 37, 201.
44. Lim, S. Y.; Tsotsis, T. T.; Sahimi, M. *J Chem Phys* 2003, 119, 496.
45. Tocci, E.; Hofmann, D.; Paul, D.; Russo, N.; Drioli, E. *Polymer* 2001, 42, 521.